# ASSESSMENT OF FATIGUE LIFE OF A STEEL GIRDER BRIDGE IN SERVICE

Fernando Cicci, De Havilland Aircraft of Canada, Ltd.; and
Paul Csagoly, Ministry of Transportation and Communications, Ontario

To assess the fatigue life of welded, cover-plated steel girders, strain gauges were placed in critical locations on the superstructure of the Leslie Street overpass on the Toronto Bypass. Data were gathered for 200 hours in 12-hour continuous tape recording sessions. Analysis of the data revealed that normal traffic caused a live-load stress peak of 4,000 psi (2757 MPa) only once in 10 hours, which is less than 50 percent design live-load stress. Stress data gathered by various agencies during the past few years seem to indicate that either design stress does not occur at all or it occurs with such a low frequency that the development of any fatigue situation is precluded. The phenomenon is associated with the low probability of the simultaneous, multiple presence of loaded commercial vehicles on a structure. The problem is therefore statistical in nature. Its recognition appears to be in conflict with the prevailing concept used in fatigue consideration of highway bridges.

•STRUCTURAL engineers in the Ministry of Transportation and Communications, Ontario, expressed considerable concern when an internal, cover-plated steel beam failed in the Yellow Mill Pond Viaduct on I-95, Bridgeport, Connecticut, in 1970. The failure originated in a crack at the toe of the fillet weld that spread along the end of the cover plate and through the flange. It had extended 16 in. (406 mm) up into the web before it was detected. Subsequent inspection revealed the presence of numerous smaller cracks at the cover plate ends at several locations in the bridge.

The ministry has a number of bridges under its jurisdication similar in construction to and built about the same time (1958) as the Yellow Mill Pond Viaduct. One of them, the Leslie Street overpass, is located on the Toronto Bypass.

The Toronto Bypass is a 12-lane artery (three core and three collector lanes in both directions) which carries 146,000 ADT (at Leslie Street), of which an estimated 13.5 percent is commercial. These figures are comparable to those obtained at the Yellow Mill Pond Viaduct (7).

The Ontario Highway Traffic Act, which controls heavy commercial vehicles in the province, permits gross vehicle weights far in excess of those in Connecticut. Five-axle tractor and semi-trailer (3S-2) combinations can carry 84,000 lb (38 000 kg) if they are conventionally constructed and 93,000 lb (42 000 kg) if they are designed in accordance with the provisions of the Ontario bridge formula (1971). In addition, eight-axle vehicle trains and five-axle special permit vehicles (usually floats transporting construction equipment) can have as much as 140,000 lb (64 000 kg) gross weight. The comparable maximum vehicle weight in Connecticut is 73,000 lb (33 000 kg).

The core section of the Leslie Street overpass consists of six simply supported spans of various lengths. The cover plates are fastened to the flanges by intermittent welds of questionable quality, which would make this structure most susceptible to fatigue cracking. [A 5,000-psi (34.47 MPa) limit for allowable range of stress $F_{sr}$ over 2,000,000 cycles is suggested (6).] The purpose of the investigation was to establish stress-range frequencies at various points of the superstructure and to predict expected service life of the bridge with available laboratory test data.

Publication of this paper sponsored by Committee on Dynamics and Field Testing of Bridges.

Figure 1. Schematic of test site.

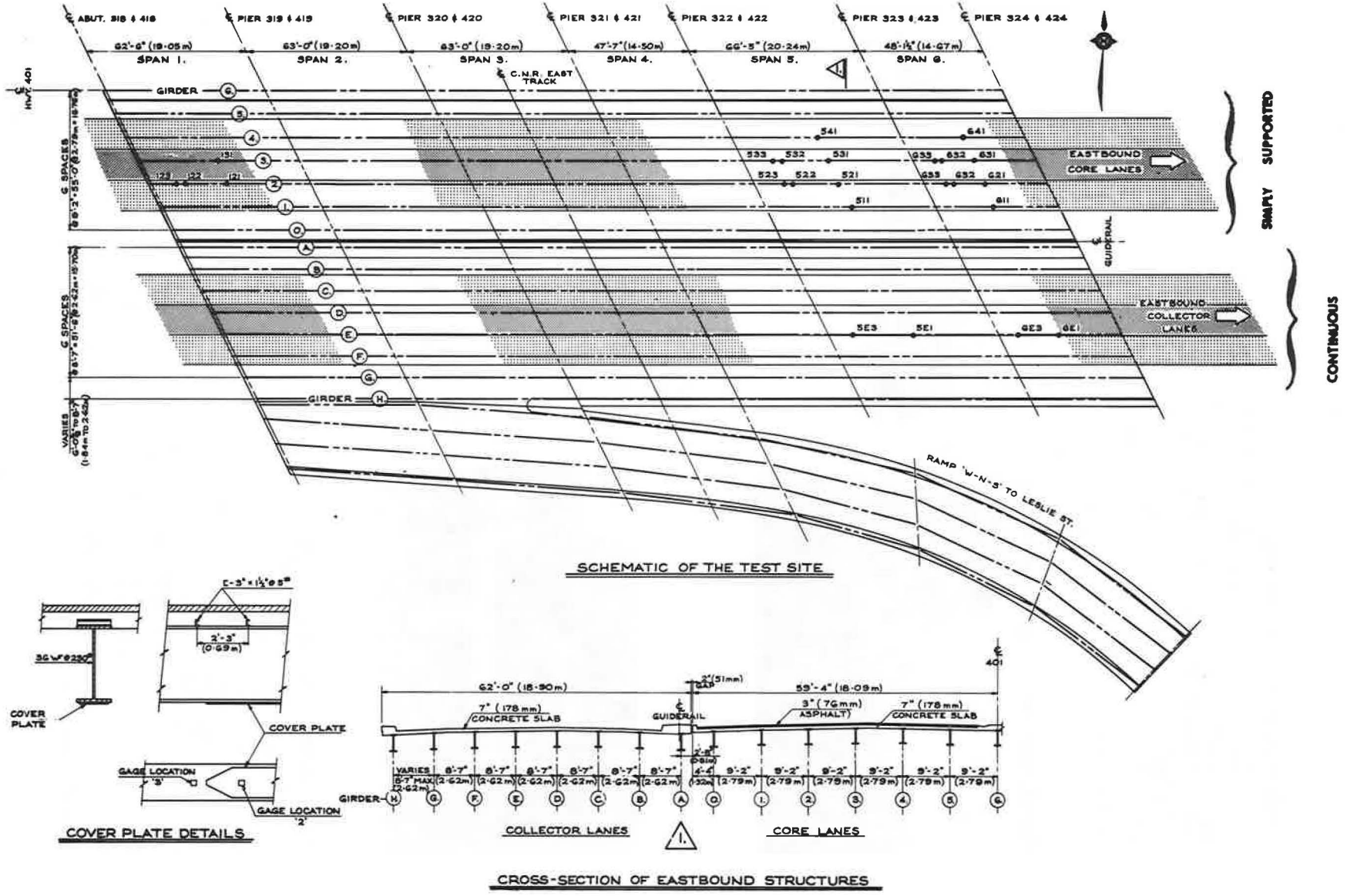

**Table 1. Girder and cover plate geometry.**

| Span Number | Bearing, Center-to-Center Distance (ft) | Beam Size | Cover Plate | | |
|---|---|---|---|---|---|
| | | | Length (ft) | Width (in.) | Thickness (in.) |
| 1, 2, 3 | 62.0 | 36WF230 | 27.5 | 14.0 | 0.375 |
| 4, 6 | 46.6 | 36WF150 | 14.5 | 10.0 | 0.375 |
| 5 | 65.5 | 36WF230 | 34.5 | 14.0 | 0.625 |

Note: 1 in. = 25.4 mm; 1 ft = 0.3048 066 m.

**Figure 2. Welding details on Leslie Street overpass.**

**Figure 3. Load-testing vehicle.**

**Figure 4. Deflectometer.**

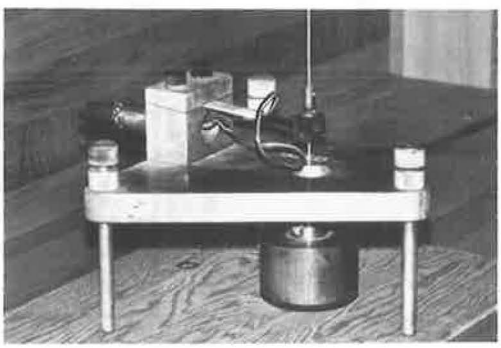

**Table 2. Placement of deflectometers (phase 1).**

| Station | Span | Beam | Position on Beam |
|---|---|---|---|
| 1 | 5 | 11 | East end of cover plate |
| 2 | 5 | 11 | Midspan |
| 3 | 5 | 11 | West end of cover plate |
| 4 | 5 | 3 | Midspan |
| 5 | 5 | 2 | Midspan |
| 6 | 6 | 3 | Midspan |
| 7 | — | — | — |
| 8 | 6 | 1 | East end of cover plate |
| 9 | 6 | 1 | West end of cover plate |
| 10 | 5 | 1 | East end of cover plate |
| 11 | 5 | 1 | West end of cover plate |

**Table 3. Deflections during test vehicle runs.**

| Run | Deflection (in.) at Station | | | | | | | | | | |
|---|---|---|---|---|---|---|---|---|---|---|---|
| | 1 | 2 | 3 | 4 | 5 | 6 | 7 | 8 | 9 | 10 | 11 |
| 1 | 0.10 | 0.08 | 0.08 | — | — | — | — | — | — | — | — |
| 2 | 0.24 | 0.23 | 0.20 | — | — | — | — | — | — | — | — |
| 3 | 0.20 | 0.19 | 0.17 | — | — | — | — | — | — | — | — |
| 4 | — | — | — | 0.17 | 0.30 | 0.07 | — | 0.12 | 0.16 | 0.22 | 0.29 |
| 5 | — | — | — | 0.33 | 0.31 | 0.18 | — | 0.06 | 0.06 | 0.11 | 0.13 |
| 6 | — | — | — | 0.21 | 0.13 | 0.08 | — | — | — | 0.06 | 0.07 |
| 7 | — | — | — | 0.12 | 0.24 | 0.08 | — | 0.11 | 0.14 | 0.16 | 0.22 |
| 8 | — | — | — | 0.23 | 0.21 | 0.17 | — | 0.04 | 0.04 | 0.08 | 0.08 |
| 9 | — | — | — | 0.13 | 0.06 | 0.08 | — | — | — | 0.02 | 0.02 |

Note: 1 in. = 25.4 mm.

This report describes the equipment used to acquire data and the methods of reducing the data to produce the required frequency distribution. An attempt has been made to apply Miner's hypothesis to predict the service life of the bridge.

## TEST SITE

The skewed bridge decks that were of interest in this test program are at the western end of the Leslie Street overpass. Figure 1 shows the six core lanes and the three eastbound collector lanes.

In the core area, which was built in 1958, each span of the structure is simply supported with the beam ends resting on neoprene bearings. There are six spans including number 1 at the extreme western end. There are three different span lengths and various girder sizes and bottom flange cover plate geometries. The combinations are given in Table 1.

Across the width of the core area there are 13 girders measuring 9 ft, 2 in. (2.79 m) from center to center. For this test program, the girders were designated 0, 1, 2, . . . , 10, 11, and $0^1$ from south to north. The 0 and $0^1$ girders were changed when the additional six collector lanes were constructed in 1965. These no longer have a welded cover plate detail and so were not considered in the measurement scheme.

Although it was believed that the welded cover plate details would be fatigue-sensitive, it was decided that a direct comparison of the stresses in another type of structure would be quite useful. The collector lanes are supported by continuous girders where the stress history in one span can be significantly influenced by a load in another. For this part of the investigation, the eight girders supporting the eastbound collector lanes on the bridge were designated A, B, . . . , and H from north to south. Figure 1 shows all girder designations and cross sections of the superstructure in the test site.

## PILOT TESTS FOR SELECTING CRITICAL LOCATIONS

All of the core lane girders in spans 1 to 6 except 0 and $0^1$ contained the welded cover plate detail. The cover plates were not welded continuously but in a series of intermittent welds as shown in Figure 2. Because a comprehensive method of analysis was lacking at the outset of the investigation, the static and dynamic live-load stresses were not known for the individual girders or along the length of each girder. Thus, the critical fatigue stress regions could not be determined a priori. To determine the most highly stressed locations, a two-phase preliminary deflection survey was initiated.

### Phase 1

Phase 1 was carried out with the ministry's structural research test vehicle (Fig. 3) loaded to a gross weight of 112,000 lb (50 000 kg). During this pilot test, the core lanes were closed to normal traffic and the bridge was traversed by the test vehicle that traveled in different lanes at two different speeds.

The deflectometers used consist of a thin wire rope firmly attached to the girder at one end and to the measuring head at the other end (Fig. 4). The measuring head is a metal tripod that rests on the ground and is connected to the wire rope through a strain-gauged cantilever. Tension in the rope is maintained with a brass weight. The deflection of the structure is then proportional to the measured strain of the centilever and can be calibrated.

The eastbound approach to the bridge is downhill and is somewhat rougher than the westbound; thus, most of the deflectometers were distributed on the girders of the eastbound core lanes. For comparison, however, three were placed under the westbound lanes. The distribution of deflectometers is given in Table 2.

Maximum deflection at each station as read from the calibrated oscillogram for each run is given in Table 3, which reveals several important facts:

1. There is little effect on the structure of the eastbound lanes by westbound traffic and vice versa.
2. The eastbound lane structure tends to deflect more than the westbound lane under nominally similar dynamic conditions. This phenomenon is believed to be associated with the difference in surface roughness.

3. As expected, girder 1 in spans 5 and 6 deflected most when the test vehicle was in the most southerly lane (runs 4 and 7, stations 8, 9, 10, and 11) because this girder is located under the right edge of the driving lane. Girder 2 is between the two right-hand lanes and, therefore, experiences equal deflection (station 5, runs 4, 5, 7, and 8). Girder 3 is under the middle lane and experiences the greatest deflection for middle-lane traffic (runs 5 and 8, stations 4 and 6).

From these considerations it was concluded that girder 2 is likely to be the most frequently and highly stressed of all the girders because it is located beneath the two right-hand eastbound lanes, which usually carry 98 percent of the heavy vehicles.

Phase 2

The second phase consisted of a continuous 2-hour monitoring of girder deflections caused by normal traffic flow. For this survey, the deflectometers were moved to new locations to concentrate on those girders that were discovered to be most active in phase 1. Three deflectometers were placed on the collector lane structure toqualitatively assess the difference in behavior between the two types of construction. The distribution of deflectometers for phase 2 is given in Table 4.

Results from the continuous monitoring confirmed an earlier observation that girder 2 experiences the most severe stressing. Figure 5 shows typical time histories (histograms) of the deflections measured during heavy vehicle passage in (a) core lanes where the maximum deflection occurs at station 5 and is about 0.164 in. (4.17 mm) and deflection at station 2 is almost as great with 0.156 in. (3.96 mm) and (b) collector lanes, which are continuous girder structures (as opposed to simply supported girders). There is an obvious coupling across the supports shown by the out-of-phase displacements of spans 5 and 6. Table 5 gives the maximum normal road traffic displacement measured at each station.

Girder 2 was expected to experience the most severe stress history. An approximate calculation of stress from deflections indicated that span 6 was expected to result in values about as high as those for spans 1 and 2, and, therefore, it was decided to investigate and monitor the three spans by using strain gauges and a magnetic tape recorder.

Twenty locations in the core lane structure and four on the collector girders were instrumented (Fig. 1). Not all of these were needed for the stress measurements; however some duplication was necessary to cover for the eventuality of gauge failures and also to allow for the possible investigation of spatial anomalies that might arise during testing.

Each strain gauge station was identified by a three-character alpha-numeric code. The first is a number designating the span. The second designates the beam and can be a number (core lanes) or a letter (collector lanes). The third is the number 1, 2, or 3 and defines the location on the beam. Number 1 designates midspan or the point of highest bending moment. Number 2 designates a station on the cover plate a few inches from its end. Number 3 designates a position on the base material 4 in. (101.6 mm) from the end of the cover plate. Table 6 gives all strain gauge stations.

## STRAIN GAUGE INSTRUMENTATION AND TECHNIQUES

Strain gauges used in the instrumentation were Micro-Measurement's EA-06-250-TG-350. The adhesive used was Micro-Measurement's AE-10, and the waterproofing compound was Automation Industries' GW-5.

The strain gauges were initially bonded with AE-10 to a 4-in.-wide (102 mm) strip of carrier material (Dupont Polymide Kapton 200H), which had been previously abraded. The gauges were wired in the full bridge configuration (Fig. 7) and waterproofed by a layer of GW-5 approximately $\frac{1}{8}$ in. (3.18 mm) thick. These patches were trimmed to 3 by 3 in. (76 by 76 mm) and installed at previously described locations on the steel girders with AE-10 adhesive, pressure pads, and heat lamps as shown in Figure 6.

A six-lead-wire system was used with two wires each for excitation, signal, and shunt calibration (Fig. 7).

**Table 4. Placement of deflectometers (phase 2).**

| Station | Span | Beam | Position on Beam |
|---|---|---|---|
| 1 | 1 | 2 | Eastern end of cover plate |
| 2 | 1 | 2 | Midspan |
| 3 | 1 | 2 | Western end of cover plate |
| 4 | 5 | 3 | Midspan |
| 5 | 5 | 2 | Midspan |
| 6 | 5 | A | Midspan |
| 7 | — | — | — |
| 8 | 5 | D | Midspan |
| 9 | 6 | D | Midspan |
| 10 | 5 | 2 | Eastern end of cover plate |
| 11 | 5 | 2 | Western end cover plate |

**Table 5. Maximum deflections during 2-hour normal traffic period.**

| Station | Maximum Deflection (in.) | Station | Maximum Deflection (in.) |
|---|---|---|---|
| 1 | 0.266 | 7 | — |
| 2 | 0.295 | 8 | 0.246 |
| 3 | 0.276 | 9 | 0.158 |
| 4 | 0.197 | 10 | 0.207 |
| 5 | 0.325 | 11 | 0.276 |
| 6 | 0 | | |

Note: 1 in. = 25.4 mm.

**Table 6. Strain gauge stations.**

| Span 1 | Span 5 | Span 6 |
|---|---|---|
| 121 | 511 | 611 |
| 122 | 521 | 621 |
| 123 | 522 | 622 |
| 131 | 523 | 623 |
| | 531 | 631 |
| | 532 | 632 |
| | 533 | 633 |
| | 541 | 641 |
| | 5E1 | 6E1 |
| | 5E3 | 6E3 |

**Figure 5. Typical road traffic girder deflections.**

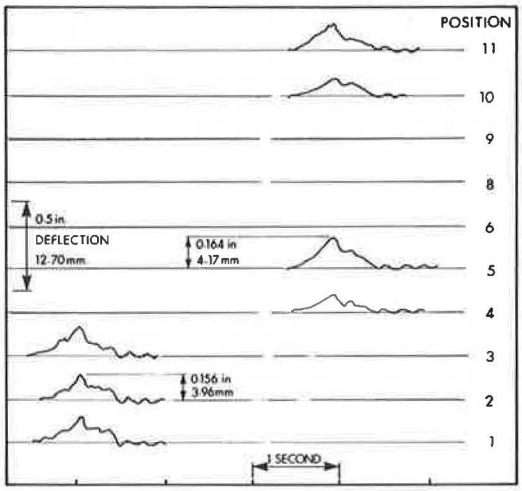


(a) HEAVY VEHICLE IN CORE LANES

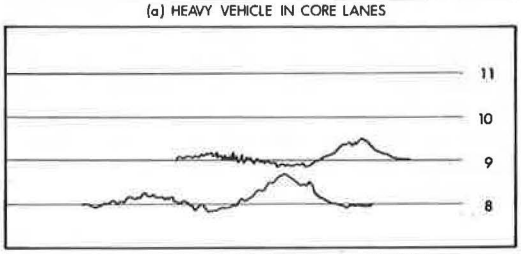


(b) HEAVY VEHICLE IN COLLECTOR LANES

**Figure 6. Strain gauge application.**

The excitation, signal conditioning, and amplification for the strain gauge bridges were supplied from an Endevco system, and the resulting signals were recorded on a seven-channel Philips Anal-Log 7 tape recorder. Calibration and zero balance adjustments were made every 12 hours during recording. The Endevco system has provision for inserting shunt calibration resistors. Suitable resistors were inserted to give calibrations of 200, 100, and 50 μin./in. (41.37, 20.68, and 10.34 MPa).

The required values of calibration resistor are calculated from the formula

$$\text{Calibration resistance} = (\text{gauge resistance}) \times \left[\frac{10^6}{\text{gauge factor} \times \text{microstrain} \times A}\right]^{-1.0}$$

where A is a bridge gain of 2.6 for the full bridge configuration used.

The resistors used were Welwyn type M22D (temperature coefficient of 100 parts per million) and had values of 316,634 and 1270 kΩ to give the required calibrations of 200, 100, and 50 ± 1 percent in all cases.

## SYSTEM TEST

Before magnetic tape recordings were begun, the strain gauge bridges were tested again with the oscillograph. A continuous recording for 1 hour was taken for each of the 24 strain gauge stations. It was found that all 24 installations were functioning satisfactorily and that each channel yielded an electronically clean and useful signal. It was decided from the preliminary deflection tests that a 200-μin./in. strain or 6,000 psi (41.37 MPa) was the maximum to be expected and that this should be used as both a maximum calibration value and a full scale for the recordings. The system test confirmed this assumption.

## STRAINS FROM PASSAGE OF A VEHICLE OF KNOWN WEIGHT

The test vehicle with a gross weight of approximately 84,000 lb (38.8 tons) was driven in normal traffic. (No attempt was made to identify the nature and distribution of commercial traffic; for obvious reasons the Toronto Bypass does not readily lend itself to such an enterprise.) The vehicle's passing time was synchronized with the tape recorder by means of a three-way radio communication. Use of the tape recorder enabled the data to be analyzed later. A total of 18 vehicle passes or runs were made.

Table 7 gives the maximum strains experienced by the bridge structure during the vehicle passage for the core lanes, and Table 8 gives those for the collector lanes.

The tabulated strains are estimated to be accurate to within approximately ±5 μin./in. or 150 psi (1.03 MPa), which allows for equipment error and manual trace interpretation. In all cases, a positive strain is tensile and a negative one compressive. The values given in Tables 9 and 10 are strictly maxima and do not give any indication of variation with time.

Figure 8 shows the core lane strain histories of stations 123 and 623 for run 8. These traces are typical of the core lane strains recorded during normal traffic flow. In some cases a slight vibratory motion was apparently induced. The preliminary study had indicated that the high-speed passes tended to yield higher deflections than the pseudostatic passes. This trend was much reduced in the strain measurements. There appeared to be little forced vibration except for the thump effect caused by the rough approach. This effect did not vary appreciably within the speed range observed.

Figure 9 shows typical strain histories for the collector lane structure. The strain gauges located on the thinned-down portion of the flange show tensile and compressive peaks in sequence. This reflects the interspan influence made possible by the continuous nature of the girders over the supports.

As in the core structure, the effect of vehicle velocity on vibration was minimal, which indicates the absence of significant forced responses. Nevertheless, the continuous structure seemed to indicate higher dynamic responses than the comparable simply supported ones that carried the core lanes.

Figure 7. Strain gauge wiring.

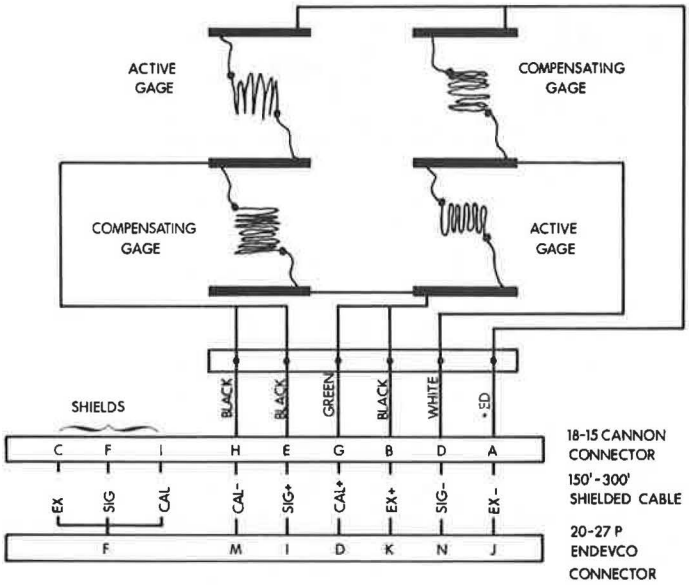


Table 7. Peak strains during passage of test vehicle (core lanes).

| Run Number | Measured Strain (μin./in.) for Station | | | | | | |
|---|---|---|---|---|---|---|---|
| | 123 | 121 | 523 | 521 | 531 | 623 | 621 |
| 2 | 85 | 69 | 55 | 57 | 33 | 59 | 54 |
| 4 | 76 | 58 | 58 | 54 | 54 | 54 | 53 |
| 6 | 21 | 21 | 20 | 20 | 35 | 21 | 18 |
| 8 | 85 | 82 | 48 | 67 | 37 | 45 | 60 |
| 10 | 72 | 57 | 50 | 54 | 60 | 84 | 68 |
| 12 | 30 | 30 | 31 | 32 | 53 | 28 | 22 |

Note: 1 μin/in. = 0.2068 MPa.

Table 8. Peak strains during passage of test vehicle (collector lanes).

| Run Number | Measured Strain (μin./in.) for Station | | | |
|---|---|---|---|---|
| | 5E3 | 5E1 | 6E1 | 6E3 |
| 13 | 15 | -19 | -18 | -19 |
| | -12 | | | 21 |
| 14 | 67 | -64 | -81 | -77 |
| | -49 | | | 100 |
| 15 | 40 | -39 | -49 | -51 |
| | -30 | | | 55 |
| 16 | 15 | -22 | -28 | -32 |
| | -15 | | | 29 |
| 17 | 69 | -78 | -87 | -85 |
| | -64 | | | 117 |
| 18 | 38 | -41 | -50 | -59 |
| | -29 | | | 53 |

Figure 8. Test vehicle induced strains at two core lane structures (run 8, Table 8).

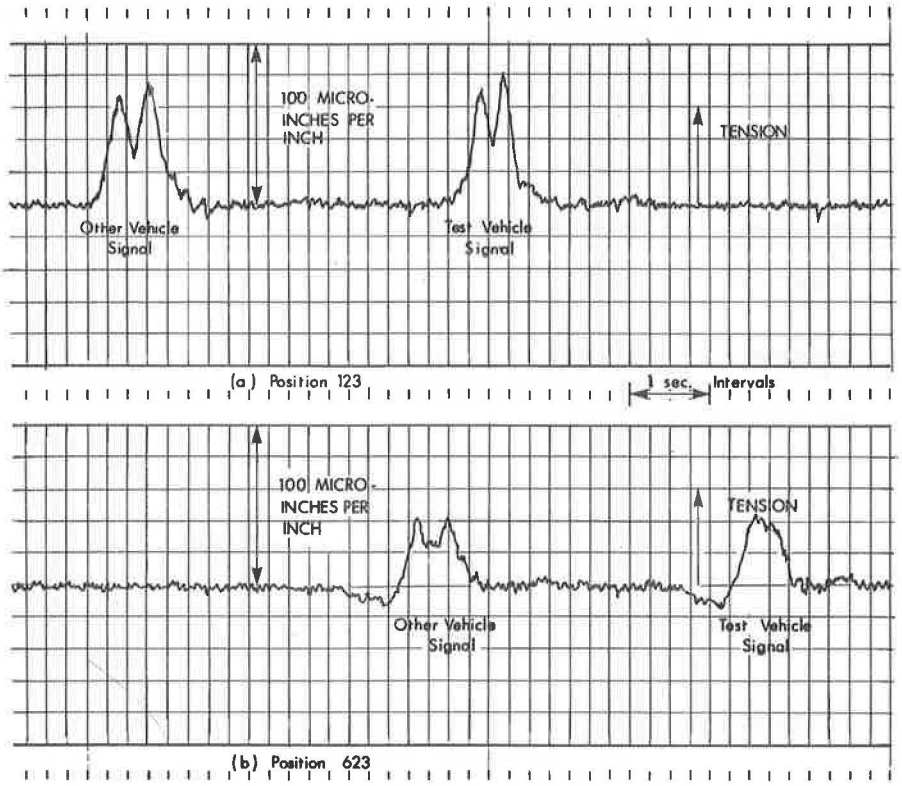


Figure 9. Test vehicle induced strains at two collector lane structures (run 17, Table 8).

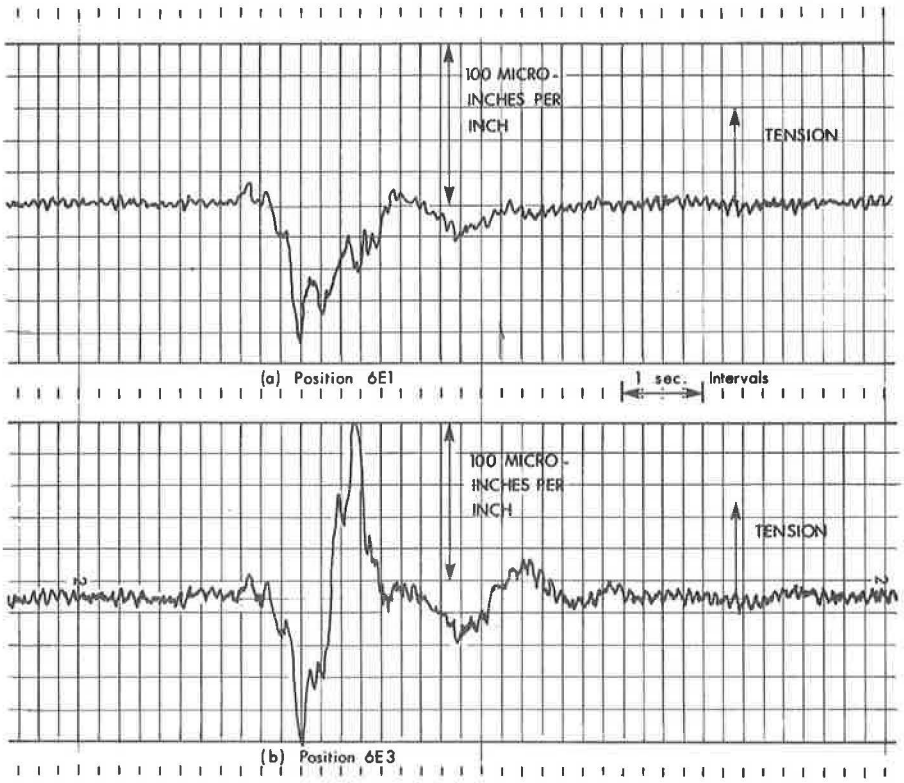

## CONTINUOUS STRAIN RECORDINGS

The continuous recording of strain began at the end of February 1972. Seven channels were recorded simultaneously. A calibration signal was recorded on each channel at the beginning of each tape for about 1 min. This was repeated at the end of the tape. All recording was carried out at the minimum recorder speed of $^{15}/_{16}$ ips (23.8 mm/s), and this resulted in a 12-hour recording for each reel of tape. The highest frequency expected in the signal was less than 5 Hz (Figs. 8 and 9), and the frequency response of the tape recorder was quite adequate at that low speed. All recordings were made in the FM mode because of the predominant low frequency of the signal.

For most of the recording session, the seven stations monitored had been found to be most severely stressed in the preliminary and system test programs. Some recordings, however, were made with signals from other stations, which were combined into groups 1 and 2.

It was decided to attempt to analyze data soon after recording and to reuse the tapes so that the required inventory of magnetic tapes could be kept to a reasonable minimum and recording continuity could be maintained. A comparison of data blocks showed that the daily traffic patterns of the Toronto Bypass are homogeneous enough to consider all data as coming from a single sample.

## DATA ANALYSIS

From the preliminary tests and the playback of the continuous records, it became apparent that the strain history was nonstationary. This precludes the more conventional means of measurement and dictates a statistical analysis.

Several parameters, such as fluctuating and mean stresses, fabrication techniques, and material, influence the fatigue life of structures. There is some indication that mean stress plays a minor role in typical materials used for built-up bridge structures that are loaded to fairly high stress levels (2). This may not be true with lower stress levels and a large number of applications. The effect of alternating stress is quite well understood for constant strain or stress fluctuations that are sinusoidal in waveform. If the time history is random in nature, stationary, and narrow banded, then the fatigue characteristics are more complex. The primary parameter, however, is the stress root-mean-squares (e.g., 3). As the bandwidth increases there is some indication that the statistical properties of the rises and falls (i.e., the magnitude of the difference between a maximum and the previous or succeeding minimum) govern fatigue characteristics (4).

Because the girder strain histories were neither sinusoidal nor stationary, a simple frequency-amplitude relationship could not be found. Therefore, calculation of the statistics of the amplitude, the maxima (peaks and troughs), and the excursion (rises and falls) would be necessary for a fatigue life assessment.

The University of Toronto computer research facility contains an eight-channel A-D interface to its IBM 360/44 digital computer. The digitizing rate is at an adequate level of 20,000 per second total for all channels. The rate chosen for the analysis was 1,250 per second per channel. Figure 10 shows an oscillograph trace at low and high paper speeds of a typical vehicle passage. A sample rate of 1,250 per second on data analysis is equal to approximately 40 per second in real time. In the lower part of Figure 10, this rate corresponds to one sample per division on the time scale, and this can be seen to give excellent resolutions or signal reproduction.

When each reel of analog tape had been digitized, it was analyzed with the IBM 360/44. The analysis consisted of several steps, which are shown in Figure 11. The data, as read by the computer, were not normalized. The calibration level and signal zero for each channel at the beginning of each tape were evaluated manually with a digital voltmeter, and these were used as input in the analysis program as initial normalizing values.

The calibration signal was rechecked at the end of each reel. In all cases it was unchanged. The signal zero, however, did change at times, which was felt to be due to (a) electronic drift, (b) temperature effects in the bridge, and (c) static load change caused, for example, by an accumulation of snow and debris on the deck during the winter.

**Figure 10. Typical vehicle strain history at low and high paper speeds for sample rate determination.**

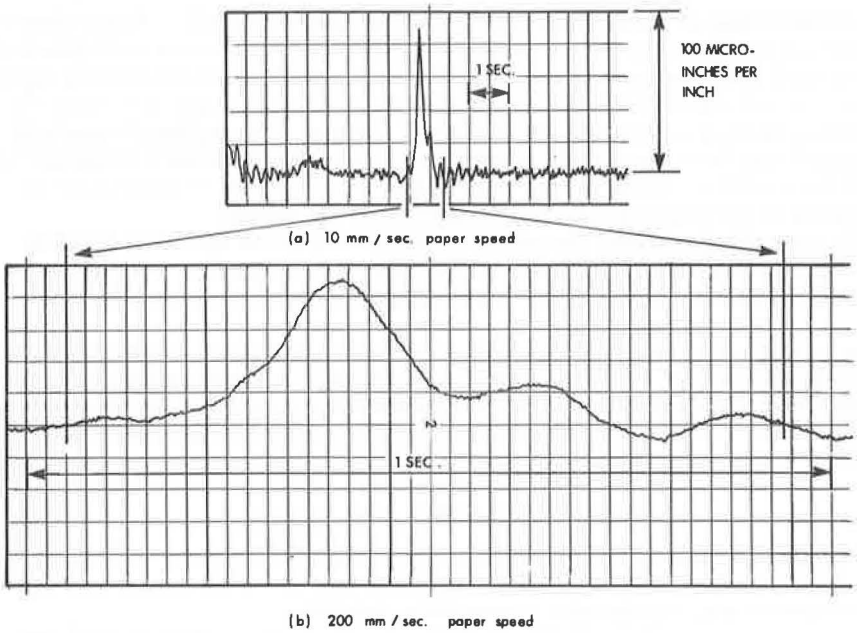


**Figure 11. Flow chart for computer analysis of digitized data.**

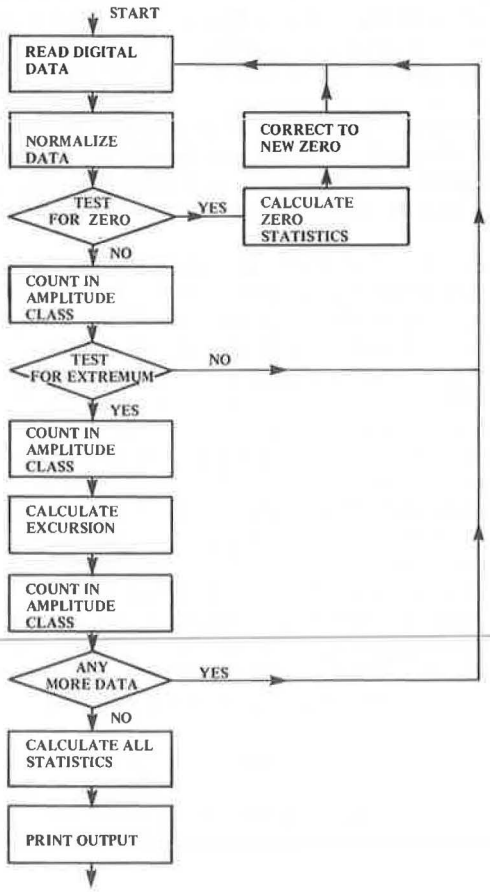

The signal zero used to compensate for these effects in normalizing was continuously updated by using the average of near zero samples. A sample was arbitrarily eliminated from the main statistical analysis if it fell between -5 and +5 μin./in (1.03 MPa) when normalized by the current factors. The mean and standard deviation of these samples were calculated as a safeguard against malfunction.

All nonzero samples, peaks, troughs, rises, and falls were tabulated by class in 5-μin./in. (1.03 MPa) increments. The mean and standard deviations for each quantity were also calculated.

The computer output on analysis consisted of one table for each channel that gave a class by class breakdown of the various statistics and a summary page listing the total counts and calculated statistics. Figure 12 shows the definition of various terms of reference used in the statistical analysis.

## EXPERIMENTAL RESULTS AND DISCUSSION

The first 24 hours of recording were of group 1 stations 121, 123, 521, 523, 531, 621, and 623. All seven channels were analyzed for a direct comparison between stations. The next 24 hours of recording were of group 2 locations, and again all seven were analyzed.

Figure 13 is a typical amplitude plot for group 1 stations during one 12-hour period. A comparison between stations revealed that station 123 was highest; 121 was next. Stations 521 and 621 were almost identical and were lower than 121.

A comparison between group 2 stations revealed that 511 was almost equal to 121 and that all the others were considerably lower. On the basis of these comparisons, it was decided for the remainder of the analysis to concentrate on 123, 521, and 621 as being representative of the most highly stressed locations.

Design stress values were calculated for station 123. Note that the core structure was designed as noncomposite; however, the channel type of shear connectors were provided, and the structure is believed to behave as at least partially composite for live loads. Bottom fiber stresses determined by using AASHTO specifications are (a) dead load—7.67 ksi or 256 μin./in. (53.9 MPa), (b) live load (noncomposite)—10.67 ksi or 356 μin./in. (73.5 MPa), and (c) live load (composite)—8.24 ksi or 275 μin./in. (56.9 MPa).

One can observe later that, assuming composite action, the maximum observed stress does not exceed 50 percent design live-load stress. This situation is believed to be common in all girder types of bridges designed in accordance with the AASHTO specifications and not particular to this structure.

The overall average number of samples in each 5-μin./in. (1.03 MPa) amplitude range per hour for stations 123 and 621 are shown in Figures 14 and 15. These are based on 133.63 hours of data, which is less than the total recorded.

The data (Figs. 14 and 15) are not true probability values because they have not been normalized. To find probability, one must divide by the total number of samples per hour (e.g., 1,250 × 3,600/32). This, however, results in extremely low probabilities in all regions except amplitudes near zero and is a valid situation because most of the time the strain values are near zero. For more meaning, the probability should be expressed in terms of a sample falling in a given range during the passage of a heavy vehicle. This is a complex joint probability because it involves the distribution of vehicles with time, the weight distribution with vehicles, and random lateral positioning of the vehicles.

A simpler, more intuitive approach can be used if it is assumed that the amplitude distribution is made up of samples from two populations (Fig. 16). One set of values is very narrow in the amplitude direction but contains a great many samples. This implicitly takes account of electronic noise plus the passage of passenger cars and light commercial vehicles. The other population is interesting for fatigue life assessment because it gives the probability of having a given strain amplitude during the passage of a heavy vehicle.

An approximation to this ideal approach implied the arbitrary rejection of data in the -5 to +5 amplitude range. The normalizing factor is then the total number of samples considered, and this results in a probability density curve that is displaced vertically but that is otherwise identical in shape to the amplitude distribution curve (Fig. 13).

**Figure 12. Data analysis terminology.**

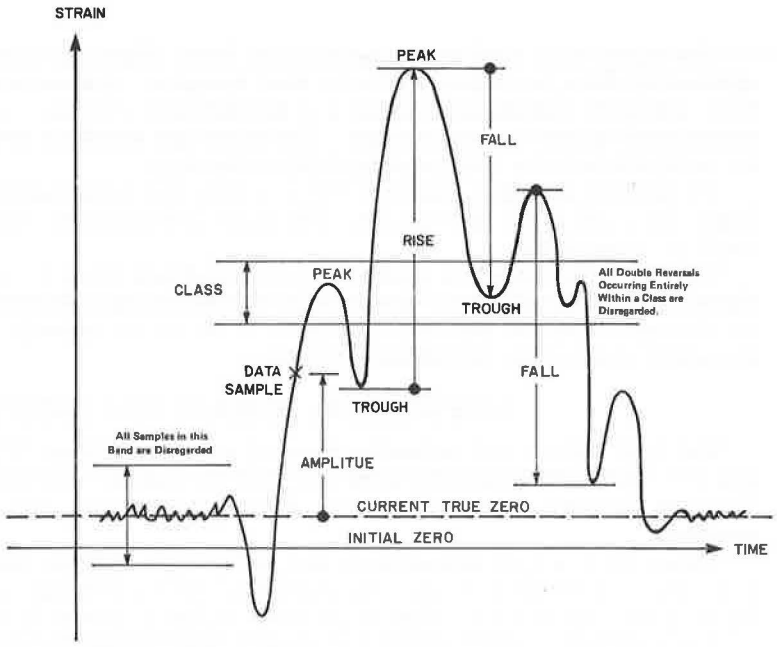


**Amplitude:** the instantaneous value of a variable or quantity.

**Peak (Trough):** a local maximum (minimum).

**Rise (Fall):** the difference in amplitude between a peak and the preceding (succeeding) trough.

**Class:** a band of arbitrary width within which all data points are considered to have equal amplitude.

**Figure 13. Strain amplitude distribution for station 621 for 11.5 hours.**

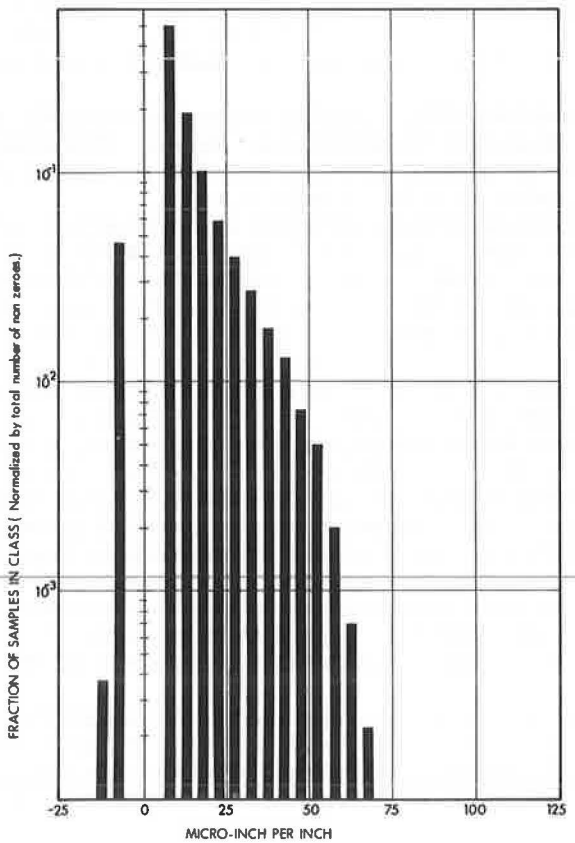

Figure 14. Strain amplitude distribution of average number of samples per hour at station 123.

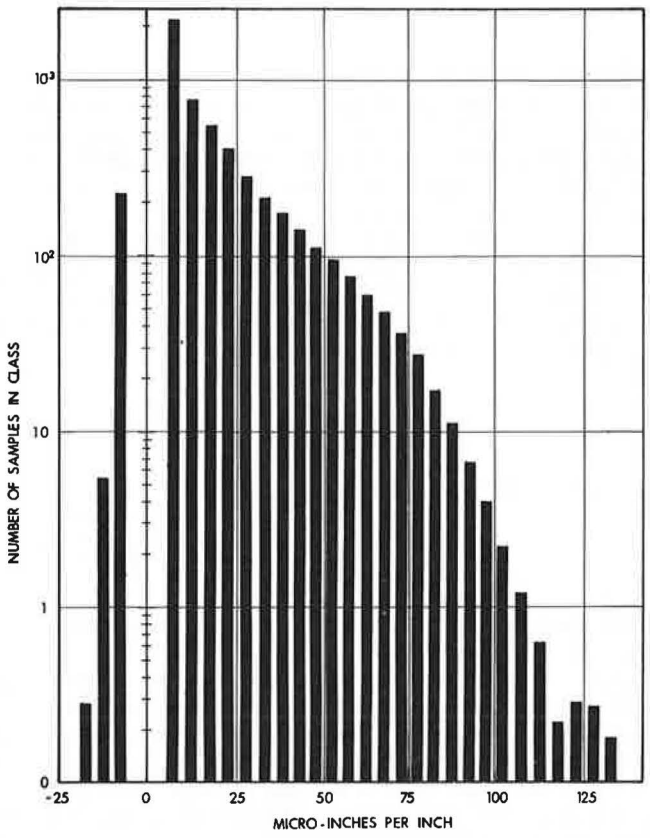


Figure 15. Strain amplitude distribution of average number of samples per hour at station 621.

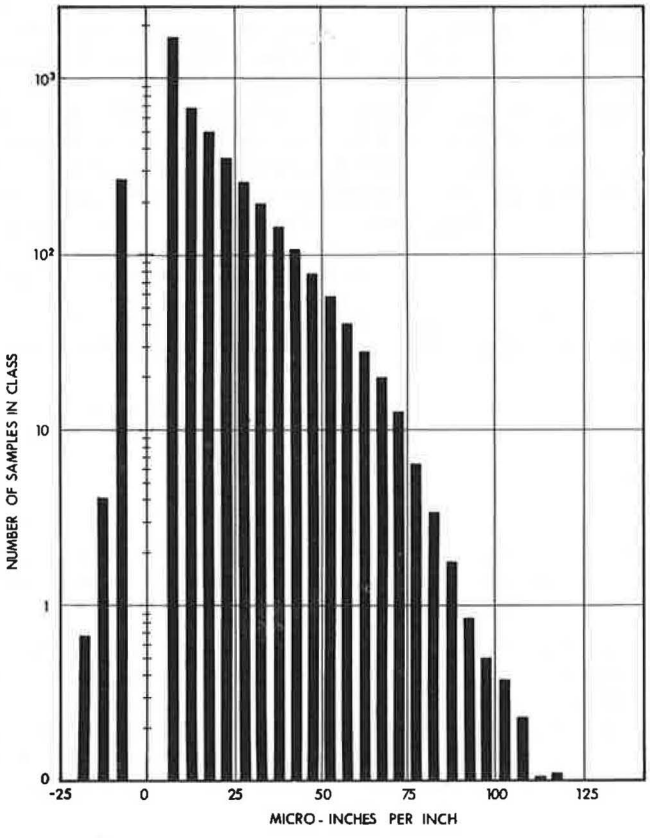

The distributions of maxima (peaks) and minima (troughs) per hour for station 123 are shown in Figures 17 and 18. As in the case of the amplitude distributions, these are not probability curves and the same considerations apply.

The distributions of excursions with amplitude are shown in Figures 19 and 20. The average hourly number of rises and falls of a given amplitude are shown, and these are almost identical to the individual quantities.

In addition to the distributions of amplitudes, extrema, and excursions, the mean and root-mean-square values are necessary for an assessment of the fatigue life. These quantities can be calculated from the distribution in the following manner: Let $a_i$ be the amplitude of the ith sample of the variable being considered and N be the total number of samples. Then the mean value is

$$\frac{\sum a_i}{N} = a$$

and the root-mean-square is

$$\sqrt{\frac{\sum (a_i - a)^2}{N}}$$

These quantities are given in Table 9 for the strain amplitude and excursions for the three critical locations.

The stress levels for the fatigue tests in Fisher et al. (2) for partial length cover plates were those on the bottom of the tension flange on the base metal at the end of the cover plate. This is exactly the configuration for station 123 in the present investigation, and, therefore, a direct comparison should be possible. However, the minimum stress range used in testing (2) was 6,000 psi (41.37 MPa), and this resulted in a life of some $7 \times 10^6$ cycles. Figure 17 shows that a stress peak of 125 μin./in. or 3,750 psi (25.85 MPa) can be expected at station 123 about once every 10 hours. A pair of excursions of that amplitude is expected about once every 24 hours (Fig. 19).

With the length of sample taken for this investigation, it is felt that the statistics are reliable to levels of extrema and excursions occurring once in 10 hours with reasonable extrapolation to once in 100 hours. As indicated above, however, even at these low levels of expectation, the measured stresses are lower than the minimum values used in other tests (2). Because of this large difference in level and of the additional major dissimilarity in waveform between the measured stresses of the Leslie Street overpass and the reported fatigue tests, a reliable quantitative prediction of fatigue life cannot be obtained. Nevertheless an attempt was made to estimate the expected fatigue life of the core lane structure by using Miner's hypothesis.

## APPLICATION OF MINER'S HYPOTHESIS

Miner's hypothesis was used to evaluate the effect of cyclic stressing of a random nature on metals. It is postulated by the following equation:

$$\sum_i \frac{n_i}{N_i} \leq 1.0$$

where

- i = index for stress range,
- $n_i$ = number of expected cycles of stress range $S_i$, and
- $N_i$ = number of cycles of stress range $S_i$ so as to cause fatigue failure as established by laboratory testing.

As a part of this investigation, the intermittent welds were exposed by sandblasting and later were inspected at many locations selected at random. No signs of fatigue cracks were found at any of these locations. This, in addition to the generally low stress levels observed, seems to indicate that the Leslie Street bridge is by no means a critical case and no great harm can be done by applying the hypothesis to the available data.

**Figure 16. Schematic example of addition of overlapping distribution.**

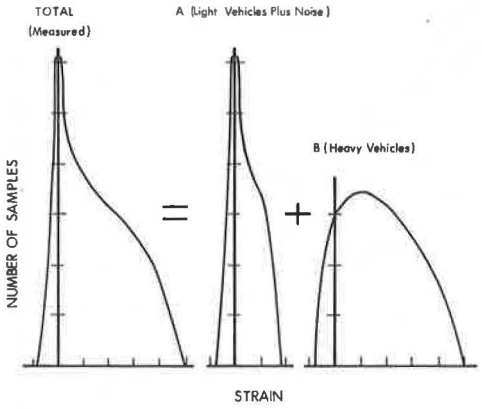


**Figure 17. Distribution of average number of maxima per hour at station 123.**

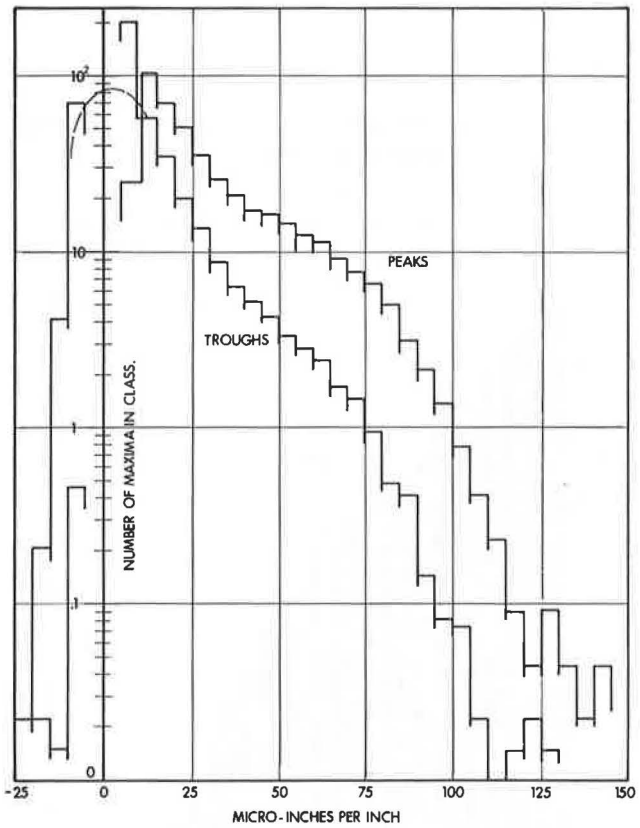

Figure 18. Distribution of average number of maxima per hour at station 521.

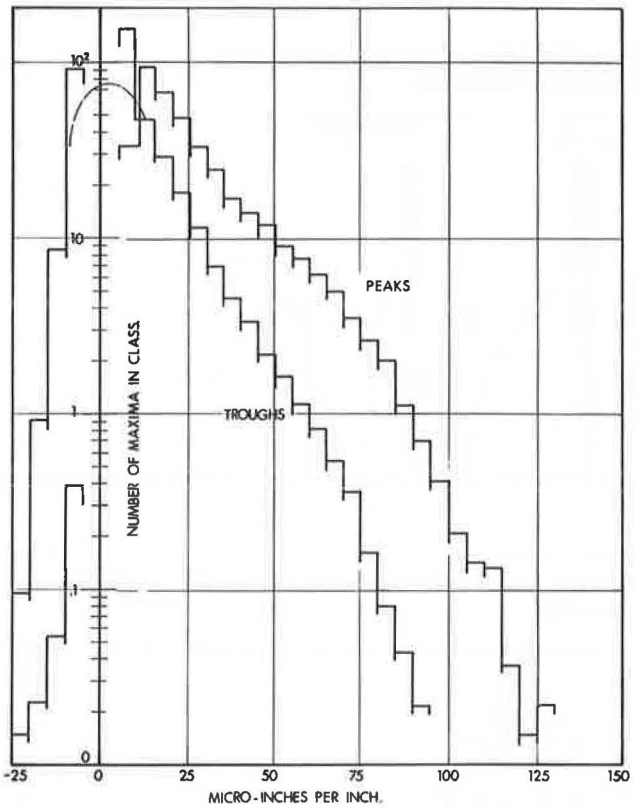


Figure 19. Distribution of average number of rises and falls per hour at station 123.

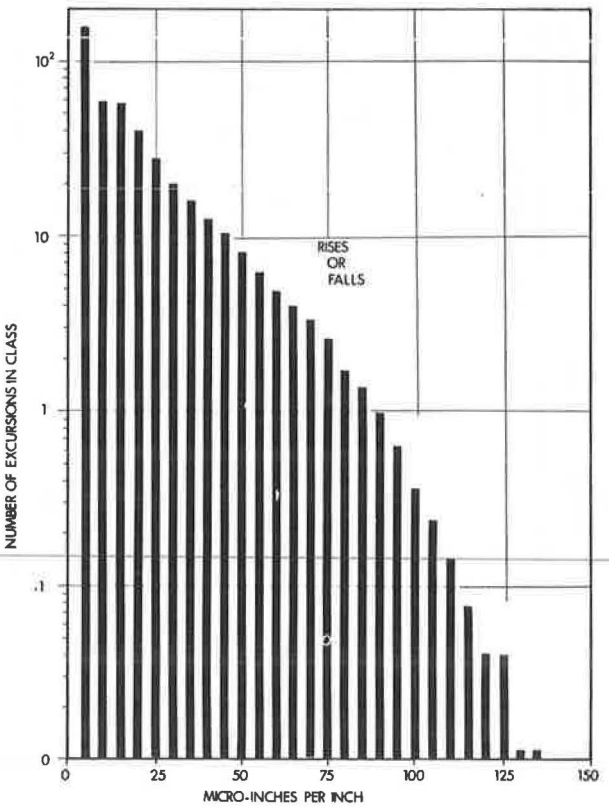

Figure 20. Distribution of average number of rises and falls per hour at station 521.

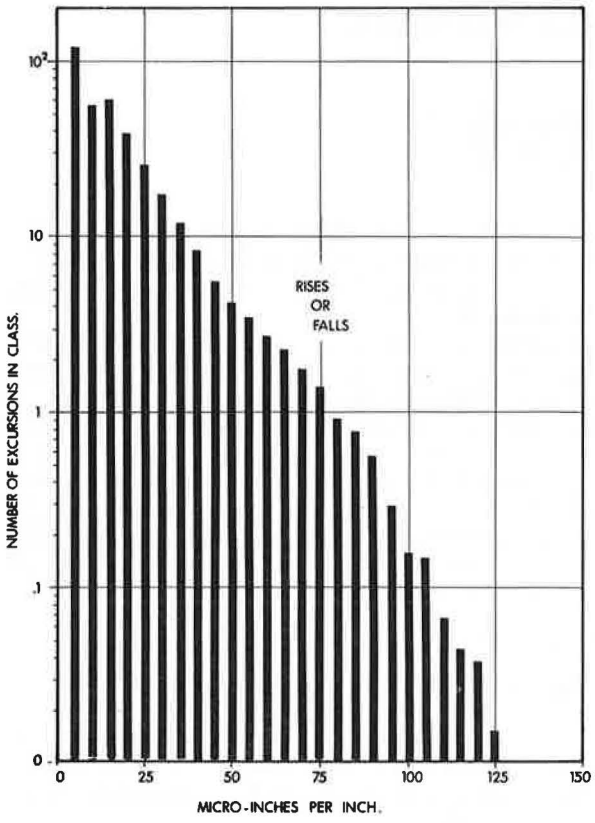


Table 9. Calculated mean and rms strains.

| | Strain Amplitude (μin./in.) | | Excursions (μin./in.) | |
|---|---|---|---|---|
| Position | Mean | RMS | Mean | RMS |
| 123 | 18.6 | 17.4 | 18.5 | 17.5 |
| 521 | 16.4 | 14.9 | 17.0 | 15.1 |
| 621 | 16.4 | 14.0 | 18.1 | 16.2 |

Figure 21. Mean fatigue strength and 95 percent confidence limits for rolled, welded, and cover-plated beams.

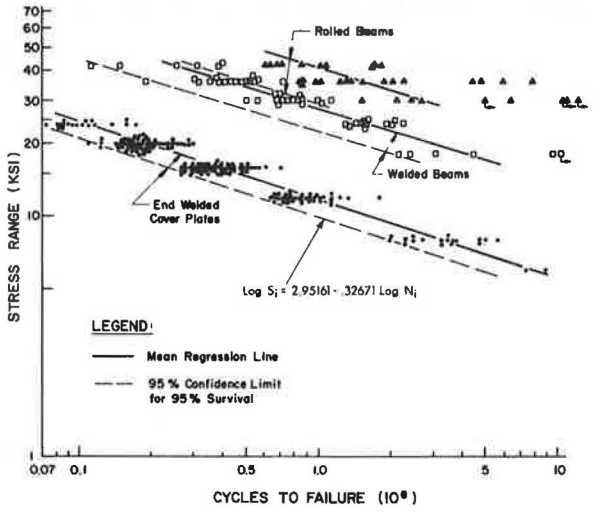


Table 10. Evaluation of data.

| Location | Expected Life (years) |
|---|---|
| 123 | 302 |
| 521 | 492 |
| 621 | 557 |

For this application the representative lower bound $S_i$ - $N_i$ curve (95 percent confidence limit for 95 percent survivals, 2) was used (Fig. 21). The equation is

$$\log S_i = 2.95161 - 0.32671 \log N_i$$

or

$$N_i = \left(\frac{894.56}{S_i}\right)^{3.06082}$$

where $S_i$ is given in ksi.

All data for this relationship were obtained for stress levels higher than 6,000 psi (41.37 MPa) and had to be extrapolated for the 0 to 4,000 psi (0 to 27.57 MPa). The validity of this extrapolation is questionable. Table 10 gives a summary of the evaluation based on 6-day weeks on a year-round basis.

If one accepts these figures for the expected life only as indicative, the margin of safety against fatigue failure still appears to be excessive. The discrepancy originates from the fact that the fatigue consideration is applied to the design live-load stress (AASHTO specifications). When one reviews the available stress history data gathered by various agencies during the past few years, it becomes evident that in reality either design stress does not occur at all or it occurs with such a low frequency that the development of any fatigue situation is precluded. The phenomenon is associated with the low probability of the simultaneous, multiple presence of vehicles on a structure. Because the problem is statistical in nature, its recognition appears to be in conflict with the prevailing concept used in fatigue consideration of highway bridges.

## REFERENCES

1. Cudney, G. R. Stress Histories of Highway Bridges. Jour. Structural Division, Proc. ASCE, Dec. 1968.
2. Fisher, J. W., Frank, K. H., Hirt, M. A., and McNamee, B. M. Effect of Weldments on the Fatigue Strength of Steel Beams. NCHRP Rept. 102, 1970.
3. Swanson, S. R. Random Load Fatigue Testing: A State of the Art. Materials Research and Standards, Vol. 8, No. 4, April 1968.
4. Rice, J. R., Paris, P. C., and Beer, F. P. On the Prediction of Some Random Loading Characteristics Relevant to Fatigue. In Acoustical Fatigue in Aerospace Structures, Syracuse Univ. Press, 1965.
5. Bendat, J. S., and Piersol, A. G. The Measurement and Analysis of Random Data. John Wiley, 1966.
6. Fatigue Strength of Welded Steel Beams. NCHRP Research Results Digest 44, March 1973.
7. Bowers, D. G. Loading History, Span No. 10 Yellow Mill Pond Bridge, I-95, Bridgeport, Connecticut. Connecticut Dept. of Transportation, Jan. 1973.